IOP Publishing European Journal of Physics
Eur. J. Phys. **43** (2022) 045601 (13pp) https://doi.org/10.1088/1361-6404/ac41d7

Relativistic velocity addition from the geometry of momentum space

Angel Paredes[1,*], **Xabier Prado**[2] and **Jorge Mira**[3]

[1] Departamento de Física Aplicada, Campus de As Lagoas, 32004 Ourense, Spain
[2] Departamento de Didáctica das Ciencias Experimentais, Facultade de Ciencias da Educación, Universidade de Santiago de Compostela, 15782 Santiago de Compostela, Spain
[3] Departamento de Física Aplicada, Facultade de Física, Universidade de Santiago de Compostela, 15782 Santiago de Compostela, Spain

E-mail: angel.paredes@uvigo.es, xabier.prado@gmail.com and jorge.mira@usc.es

Received 14 July 2021, revised 25 November 2021
Accepted for publication 10 December 2021
Published 2 May 2022

Abstract

With the goal of developing didactic tools, we consider the geometrization of the addition of velocities in special relativity by using Minkowski diagrams in momentum space. For the case of collinear velocities, we describe three ruler-and-compass constructions that provide simple graphical solutions working with the mass-shell hyperbola in a $1+1$-dimensional energy–momentum plane. In the spirit of dimensional scaffolding, we use those results to build a generalization in $1+2$ dimensions for the case of non-collinear velocities, providing in particular a graphical illustration of how the velocity transverse to a boost changes while the momentum remains fixed. We supplement the discussion with a number of interactive applets that implement the diagrammatic constructions and constitute a visual tool that should be useful for students to improve their understanding of the subtleties of special relativity.

Keywords: special relativity, education in physics, geometrical methods

(Some figures may appear in colour only in the online journal)

1. Introduction

Special relativity is one of the cornerstones of modern physics and it has been an essential underlying formalism for many scientific and technological breakthroughs. However, since the typical velocities found in daily experience are much smaller than the speed of light, it is not

*Author to whom, any correspondence should be addressed.

easy to develop correct intuitions when first getting acquainted with the subject. Plenty of learning difficulties have been reported for students facing the topic both at the secondary school and undergraduate levels, see [1, 2] for recent literature reviews. Thus, developing didactic tools for concepts of this century-old theory remains useful and interesting.

A particularly compelling perspective is that of emphasizing the utilization of graphics and visual tools to complement the more standard approach based on equations. The convenience of representing relativistic phenomena in plots has been clear since Minkowski introduced his spacetime diagrams soon after Einstein formulated the theory. More recently, several authors have followed this kind of visual path to the didactics of relativity, see for instance [3–5] for enlightening discussions. Another interesting contribution is [6], where the author put forward the pedagogical usefulness of Minkowski diagrams in momentum space to analyze the kinematics of relativistic collisions. Several aspects of the approach were later studied in more detail in [7, 8].

Our main goal is to show that Minkowski diagrams in momentum space are also well suited to provide illustrative visual displays for another basic aspect of special relativity, the addition of velocities. The geometrization of the velocity addition formulas has been addressed in two beautiful papers, [9, 10]. However, the methods of [9, 10] rely on the definition of auxiliary geometrical objects, circles and spheres, that do not have a clear interpretation in the framework of special relativity. By working directly in momentum space with mass-shell hyperbolas, we present an alternative perspective on the problem, opening new possibilities for the students' learning process. By relating aspects of the geometry of hyperbolas with basic results of spacetime dynamics, we hope that we can also contribute to the amusement of the knowledgeable reader.

In order to make clear what is the question at hand and to fix notation, let us formulate the problem. Suppose an object A (e.g. a train) is moving with velocity $\mathbf{v_A}$ with respect to a particular inertial frame of reference S (e.g. the rails). A second object B (e.g. a passenger walking in the train) is moving with velocity $\mathbf{v_B}$ with respect to A. We want to know the velocity of the object B with respect to S, which we will call $\mathbf{v_C}$. Notice that the same problem can be rephrased as the change of reference frame from S' (the inertial frame in which the object A is at rest) to S, produced by a boost of velocity $-\mathbf{v_A}$. In section 2 we address the case in which $\mathbf{v_A}$ and $\mathbf{v_B}$ are parallel and in section 3 we generalize the discussion to the non-parallel situation.

Furthermore, in order to supplement the reading of this paper, we have developed a series of interactive applets that can be easily accessed through the internet [11]. These applets, presented in section 4, show the constructions of sections 2 and 3, allowing the reader to modify the parameters and to see how the results change. This kind of virtual visual tools are interesting for students since they can enhance their learning process and can help in engaging and motivating them, see [12, 13] and references therein. Moreover, they are particularly well-suited for remote learners [14], a fact that is particularly relevant in these years when online education has greatly expanded throughout the world.

Before entering the technical discussion, it is important to put in perspective the methods that will be discussed below. One of the most fundamental issues to be understood about special relativity is that of Lorentzian geometry in Minkowski space. In fact, the results for the relativistic composition of velocities arise naturally in that framework. However, it is easier to develop visual intuitions working in Euclidean geometry, especially for neophytes. Thus, we will base our analysis on an auxiliary Euclidean geometry that can be built by choosing a particular inertial reference frame, to which the constructions refer and which should be understood as

providing an additional input to build the plots[4]. It is in that sense that we can define the orthogonal energy–momentum system of coordinates and define ordinary angles in the $E - p$ plane. In this context, we hope that our analysis will supply a useful additional viewpoint on the important topics of velocity addition and reference frame boosts. It provides geometrical tools and an amusing playground where to work with relativistic concepts. Nevertheless, it should be understood that this perspective can complement, but cannot substitute, more standard approaches based on Minkowski geometry, which, being fundamental for special relativity, students must undoubtedly comprehend to fully grasp the subtleties of this beautiful theory[5].

2. Geometrical representation of velocity addition in 1 + 1 dimensions

In this section we restrict the problem to the case in which both velocities are parallel and the interesting dynamics takes place in the temporal dimension and just one spatial dimension. Since in this case their vectorial nature is inconsequential, we will just denote the velocities as v_A, v_B. In Galilean physics, the answer would of course be simply $v_C = v_A + v_B$. However, this is in clear contradiction with the postulate of special relativity asserting that the speed of light c is independent of the motion of the emitting body, namely $v_C = c$ if $v_B = c$, independently of the value of v_A. The well-known expression for the relativistic velocity addition in $1 + 1$ dimensions, first discovered by Poincaré, is [15] (from now on, we will use natural units $c = 1$):

$$v_C = \frac{v_A + v_B}{1 + v_A v_B}. \tag{1}$$

A useful way of rewriting this expression is [3]:

$$\frac{1 - v_C}{1 + v_C} = \frac{1 - v_A}{1 + v_A}\frac{1 - v_B}{1 + v_B}. \tag{2}$$

(Notice that in this collinear case this expression can be interpreted in terms of the relativistic Doppler effect that states that the ratio of frequencies in different frames is $\sqrt{\frac{1+v}{1-v}}$ and therefore equation (2) yields $\frac{\nu''}{\nu} = \frac{\nu''}{\nu'}\frac{\nu'}{\nu}$.) Our goal is to provide a novel geometric perspective on the velocity addition formula (1). With that purpose, we will represent a series of Minkowski diagrams in momentum space [6]. The relation of energy and momentum with velocity for a body of mass m are:

$$E = m\gamma, \qquad p = m\gamma v, \qquad \text{with} \quad \gamma = \frac{1}{\sqrt{1 - v^2}} \tag{3}$$

and therefore a particle of mass m is represented by its mass shell hyperbola $E^2 - p^2 = m^2$. We can define the hyperbolic angle ϕ by parameterizing $E = m\cosh\phi$, $p = m\sinh\phi$ such that $v = p/E = \tanh\phi$. From this definition it is immediate to check that $e^{-2\phi} = \frac{1-v}{1+v}$ and the velocity addition formula (1) corresponds simply to a sum of hyperbolic angles $\phi_C = \phi_A + \phi_B$. This makes obvious the usefulness of equation (2) and the introduction of ϕ. Since it is well known

[4] As a technical note for experts, this Euclidean metric with respect to an inertial observer can be written in covariant form as $\eta_{\mu\nu} + 2u_\mu u_\nu$ where $\eta_{\mu\nu}$ is the Minkowski metric in mostly plus convention and u_μ the normalized timelike direction of the observer. In this way, in the frame in which the observer is static, we have $\mathrm{d}s_E^2 = (-\mathrm{d}t^2 + \mathrm{d}\mathbf{x}^2) + 2\mathrm{d}t^2 = \mathrm{d}t^2 + \mathrm{d}\mathbf{x}^2$. Let us also point out that both Minkowskian and Euclidean geometries are flat (in the Riemannian sense), allowing for the definition of global parallelism, that is essential for our discussion.

[5] We gratefully thank an anonymous referee for emphasizing the questions discussed in this paragraph.

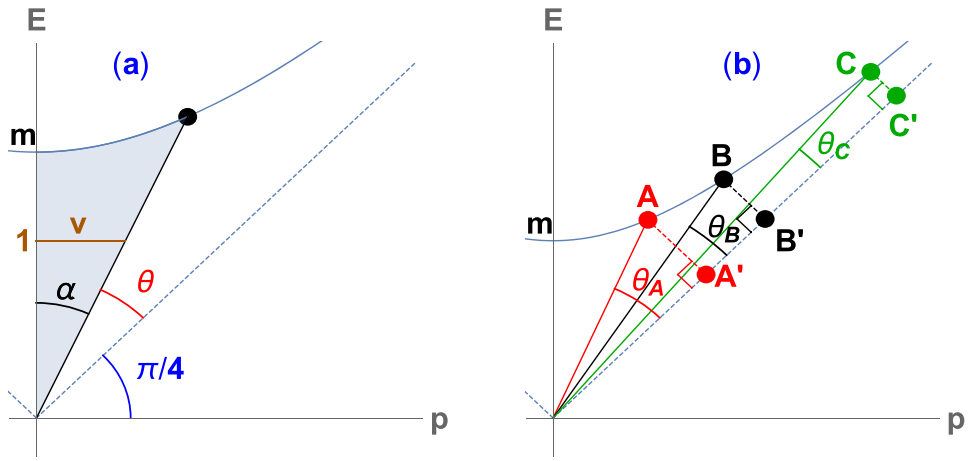

Figure 1. In plot (a), the blue solid line represents the mass shell hyperbola for a given m and the dashed lines correspond to the light cone $E = |p|$. The shaded area is proportional to the hyperbolic angle ϕ defined in the text (more precisely, the area is $\frac{1}{2}m^2\phi$). We also define the angles α and θ. The horizontal line is a measure of the velocity in terms of the scale defined by the 1 in the vertical axis. In plot (b), we depict an example of a solution of the velocity addition formula expressed as in equation (7). For later use, we also define A', B', C' as projections onto the light cone ($\overline{AA'}$, $\overline{BB'}$, $\overline{CC'}$ are perpendicular to the $E = p$ line).

that the hyperbolic angle is proportional to the shaded area depicted in figure 1(a), we can conclude that equation (1) can be rephrased as a sum of such shaded areas. However, this somewhat trivial geometrization of (1) hardly provides any visual insight on the problem. Our real aim is to find more intuitive and didactic geometrical realizations of equation (1) and, for that reason, in figure 1(a) we also define angles α and θ, which for any momentum p are given by[6]:

$$\tan\,\alpha = \frac{p}{E} = v, \qquad \theta = \frac{\pi}{4} - \alpha. \tag{4}$$

We have also defined a scale '1' on the vertical line such that, according to equation (4), the horizontal segment from the vertical axis to the solid line is precisely v. This is a kind of 'ruler for velocities' in the energy–momentum plot. We will not plot it in the rest of figures to avoid confusion with too many lines but one should keep in mind this quantitative way of graphically determining the velocity once a point in the $p - E$ plane is known.

We now look for a simple relation between angles that solves the addition of velocities. Using the trigonometric identity:

$$\tan\left(\frac{\pi}{4} - x\right) = \frac{1 - \tan\,x}{1 + \tan\,x} \tag{5}$$

we immediately find that

$$\tan\,\theta = \frac{1 - v}{1 + v} \tag{6}$$

[6] Notice that we have related a hyperbolic angle and an ordinary angle to the velocity, $v = \tanh\,\phi = \tan\,\alpha$. Recalling the relation $\tanh(ix) = i\tan x$ and that $v = \mathrm{d}x/\mathrm{d}t$, this shows the interest of defining a 'complex time' it that links the Euclidean and Minkowskian presentations.

and therefore we can rewrite the velocity addition formula (2) as:

$$\tan\,\theta_C = \tan\,\theta_A\,\tan\,\theta_B. \tag{7}$$

The angles for a particular case are depicted in figure 1(b).

Notice that $\theta \in [0, \pi/2]$ and therefore the tangents are positive numbers. Negative velocities correspond to $\pi/4 < \theta \leqslant \pi/2$. Let us comment on how basic features of the velocity addition formula are apparent from equation (7). First, since $v = 1$ corresponds to $\tan\theta = 0$ and $v = -1$ corresponds to $\tan\theta = \infty$, it is clear that the velocity found by combining any number of velocities in the $-1 < v < 1$ interval will still produce a velocity within the same interval. Moreover the product of $\tan\theta = 0$ with any other $\tan\theta$ will remain zero, meaning that adding the speed of light to any other velocity will remain the speed of light. The same is obviously true for $v = -1$, $\tan\theta = \infty$. The exception is the ill-defined case of adding $v = -1$ and $v = 1$, which produces an indetermination, as expected. Following [10], we may also wonder what would be the result if we allow for tachyonic velocities $|v| > 1$. They would correspond to $\tan\theta < 0$. Thus adding a tachyonic velocity with a subluminal one would remain tachyonic whereas adding two tachyonic velocities results in a subluminal one, in agreement with [10].

It is also worth commenting on the role of the mass shell hyperbola. It can be illustrative for students to see that different points in the same hyperbola can correspond to different states of motion with respect to a particular reference frame or to the same state of motion as seen by different observers. Finally, notice that the velocity v_A, as defined above, is a relative velocity between reference frames and not a velocity of the body of rest mass m and, thus, the point A of the figure does not really correspond to a physical motion of the body. However, since the relation between velocities and angles in equation (4) does not depend on m, it can be depicted in the same plot.

Let us now take an extra step and show how the point C can be found from the diagram with three simple ruler-and-compass constructions, once the hyperbola, A and B are given. We analyze in turn both types of constructions.

For the first construction, consider the projection of A and B on the light cone to find the points A' and B', as depicted in figure 1(b). We also define M as the rest point on the hyperbola and its projection M'. The length OA of the segment $\overline{OA}$ is:

$$OA = \sqrt{E_A^2 + p_A^2} = m\sqrt{\gamma_A^2 + v_A^2\gamma_A^2} = m\sqrt{\frac{1+v_A^2}{1-v_A^2}}. \tag{8}$$

From equation (4), it is straightforward to check that $\cos\,\theta = \frac{1+v}{\sqrt{2}\sqrt{1+v^2}}$ and therefore we can find $OA' = OA\cos\theta$ and similarly OB' and OM':

$$OA' = m\sqrt{\frac{(1+v_A)}{2(1-v_A)}}, \qquad OB' = m\sqrt{\frac{(1+v_B)}{2(1-v_B)}}, \qquad OM' = \frac{m}{\sqrt{2}}. \tag{9}$$

Therefore, the velocities enter the expressions for the projections along the light cone as the inverse of the fractions appearing in equation (2). This allows us to rephrase the velocity addition formula (2) in terms of products of these segment lengths.

$$OC' = OA'\;OB'/OM'. \tag{10}$$

We can solve this equation graphically using the trick depicted in figure 2(a). First, we find B'' and M'' as the mirror images of B' and M' with respect to the vertical axis. Then, we draw the segment $\overline{M''A'}$ and a parallel to this segment from B'', that cuts the $E = p$ line at C'. Noticing

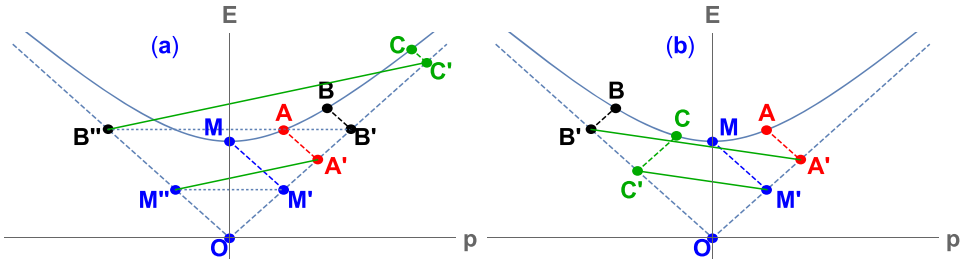

Figure 2. In plot (a), we display the ruler-and-compass construction based on Thales' theorem for similar triangles that allows us to graphically determine the position of C' and then C, thereby solving the relativistic addition of velocities. In plot (b), we depict a solution when v_A and v_B have different signs.

that $OM' = OM''$ and $OB' = OB''$ and that the triangle $OB''C'$ is similar to $OM''A'$, Thales' theorem ensures the relation (10).

An analogous but even simpler graphical procedure also leads to the solution of the velocity addition in the case in which v_A and v_B have opposite signs, see figure 2(b). For the example, let us assume $v_B < 0$, $v_A > 0$ and $|v_B| > v_A$. In this case, the expression of OB' in equation (9) has to be modified to

$$OB' = m\sqrt{\frac{(1 - v_B)}{2(1 + v_B)}}. \tag{11}$$

The easiest way to understand this is to realize that, in fact, $OB' = m\sqrt{\frac{(1+|v_B|)}{2(1-|v_B|)}}$, and similarly for OA' and OC'. Taking this into account, the equivalent of equation (10) is $OC' = OB'\, OM'/OA'$. The construction depicted in the figure ensures this equality due to the similarity of the $OC'M'$ and $OB'A'$ triangles.

The second ruler-and-compass construction is shown in figure 3(a). First define the point $-A$ as the reflection of A to negative momenta. Then, draw from $-A$ the parallel to the $\overline{MB}$ segment and the result is the point where it cuts the hyperbola[7]. Analytically, this can be proven by requiring that the slopes of the parallel segments are equal, $\frac{E_B - m}{p_B} = \frac{E_C - E_A}{p_C + p_A}$, and thus:

$$\frac{\gamma_B - 1}{v_B\gamma_B} = \frac{\gamma_C - \gamma_A}{v_C\gamma_C + v_A\gamma_A}. \tag{12}$$

This expression can be shown to be equivalent to equation (1). However, a maybe more intuitive way of thinking of this construction is that it relies on a graphical way of adding hyperbolic angles, which can be found by analogy with a similar procedure for ordinary angles, shown in figure 3(b).

[7] In fact, once the position in the $p - E$ plane of A and B are known, the point C can be determined with ruler and compass even without having the hyperbola. This is because a straight line connecting the midpoints of two parallel chords of a hyperbola passes through the center and, thus, the green dashed line of figure 3(a) bisects the chords. Taking that into account and drawing the parallel to the $\overline{BM}$ segment through $-A$, the position of C is immediately found. A similar comment applies to the construction described in figure 4.

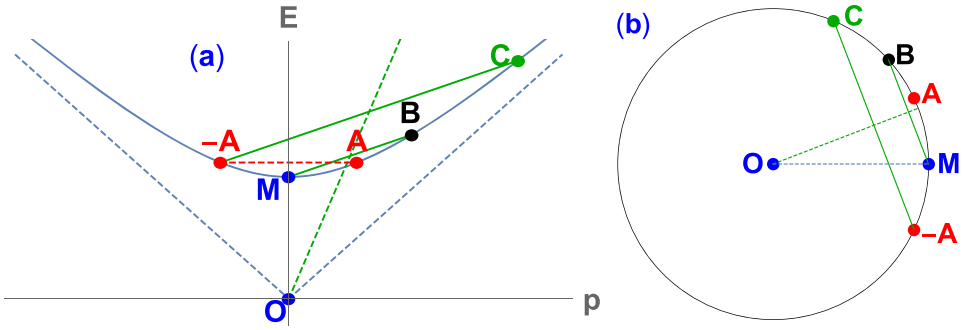

Figure 3. In plot (a), we show a simple graphical construction for the addition of hyperbolic angles and therefore for the relativistic addition of velocities. In plot (b), we show the analogous construction for the addition of ordinary angles. The chords joining B with M and $-A$ with C are parallel and the line through their middle points therefore passes through the center. This shows that the arcs from B to C and from $-A$ to M are equal. This then implies that the arc MC is MA plus MB. In both figures, the green dashed line bisects the parallel chords.

Actually, there exists an even simpler construction without need of any auxiliary points[8]. In fact, the segments $\overline{AB}$ and $\overline{MC}$ are parallel, as can be proved by verifying that:

$$\frac{E_B - E_A}{p_B - p_A} = \frac{E_C - m}{p_C}. \tag{13}$$

This is graphically depicted in figure 4. In the same figure, we reinsert the 'ruler for velocities' defined in figure 1 by inserting an arbitrary scale that we identify with 1. Then, the quantitative relation between v_A, v_B, v_C and c can be directly read along the horizontal axis.

In summary, we have provided visual representations of the velocity addition formula in $1+1$ dimensions by presenting four geometrical versions of it working in momentum space:

- The sum of shaded areas as the one of figure 1(a).
- The trigonometric identity (7), with the angles as represented in figure 1(b).
- A ruler-and-compass construction based on equation (9) and Thales' theorem for similar triangles, see figure 2.
- Two ruler-and-compass constructions for the addition of hyperbolic angles, figures 3 and 4.

Notice that the first and fourth representations rely on the fact that velocity addition is equivalent to the addition of hyperbolic angles along the mass-shell hyperbola. On the other hand, the second and third ones are related to the formulation displayed in equation (2). The ruler-and-compass methods are the main results of this section and can be visualized with the applets described in section 4.

3. Geometrical approach to velocity addition in $1+2$ dimensions

In this section, we will address the case in which the velocities to be added, defined as in the first paragraph of section 2, are not collinear. Let us assume for simplicity that the velocity

[8] We thank an anonymous referee for pointing out this construction.

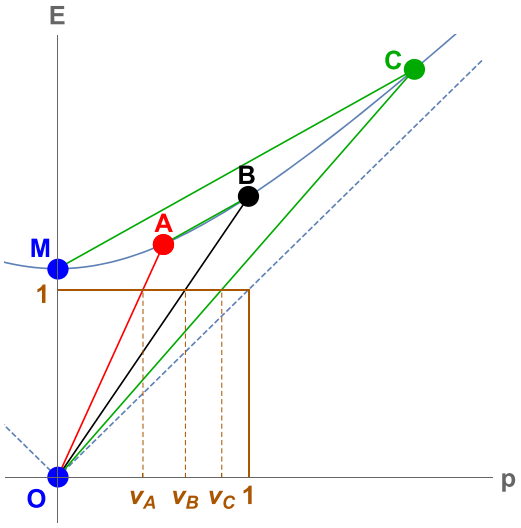

Figure 4. We show the simplest graphical construction for the addition of hyperbolic angles and therefore for the relativistic addition of velocities. A segment parallel to the $\overline{AB}$ chord is drawn from M and the point C is found from its intersection with the hyperbola. In this plot, we also explicitly depict the value of the three velocities by arbitrarily introducing a scale '1' for the speed of light along the energy and momentum axes.

$\mathbf{v_A} = (v_A, 0, 0)$ is directed along the x-axis and that $\mathbf{v_B} = (v_{Bx}, v_{By}, 0)$ lies in the x–y plane (this can always be achieved by a rotation of the Cartesian coordinates). The result of the addition of velocities in this case is not symmetric, in the sense that $\mathbf{v_A}$ and $\mathbf{v_B}$ cannot be interchanged, as a consequence of the noncommutativity of Lorentz transformations [15]. We have:

$$v_{Cx} = \frac{v_A + v_{Bx}}{1 + v_A v_{Bx}}, \qquad v_{Cy} = \frac{v_{By}\sqrt{1 - v_A^2}}{1 + v_A v_{Bx}}. \tag{14}$$

In order to represent these transformations in Minkowski diagrams in momentum space, first notice that the mass shell is a hyperboloid that is the surface of revolution of the hyperbola used in section 2, $E^2 = m^2 + p_x^2 + p_y^2$. A Lorentz transformation consisting of a boost along x leaves unchanged the transverse component of momentum, namely:

$$p_y = m v_{By}\gamma_B = m v_{Cy}\gamma_C, \tag{15}$$

where we have defined $\gamma_B = \frac{1}{\sqrt{1 - v_{Bx}^2 - v_{By}^2}}$ and similarly for γ_C. Thus, the transformation takes place in a plane of constant p_y, and, once we have reduced the problem to this plane, it is obvious that the transformation of velocity along x is exactly as in section 2, see figures 5 and 6. The intersection of the hyperboloid with the fixed p_y plane is a hyperbola whose distance to the origin is the transverse mass $m_T = \sqrt{m^2 + p_y^2}$, see figure 6(a). Looking at the geometry in this plane, one can directly follow the arguments of section 2. In fact, since the result of velocity addition does not depend on the mass, it is natural that the first equation in (14) coincides with (1). Both the identity (7) and the ruler-and-compass constructions of figures 2–4 can also be applied in this case to provide a geometrical insight on the behavior of the velocities along x.

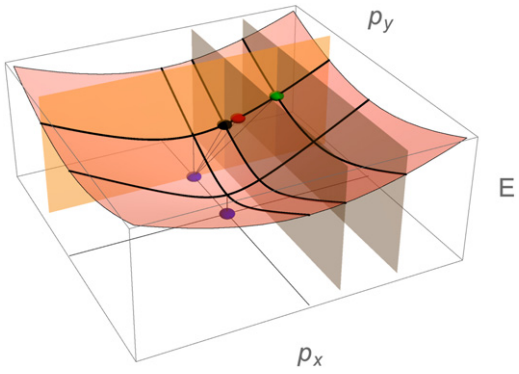

Figure 5. A three-dimensional plot in Minkowski momentum space representing the addition of non-collinear velocities. The hyperboloid represents the mass-shell of the body of mass m. Its energy and momentum with respect to S' are represented by the black dot and those with respect to S by the green dot. The red dot represents the relative velocity between frames as explained in section 2. The highlighted plane of constant p_y includes the three dots and its intersection with the hyperboloid is the hyperbola of figure 6(a). The two highlighted planes of constant p_x correspond to the momentum in both reference frames and their intersections with the hyperboloid are the hyperbolas depicted in figure 6(b). We also highlight the hyperbolas corresponding to the $p_y = 0$ and $p_x = 0$ cuts, that have also been included in figures 6(a) and (b) respectively.

Figure 6(b) provides a geometric interpretation of the change of the velocity along y even if p_y does not change: moving to a different hyperbola implies having a different angle α and therefore a different velocity.

In fact, it is possible to understand from the geometry that the change in velocity along the y-axis is precisely the one needed to maintain the y-momentum fixed when the relativistic factor γ changes due to the addition of velocities along x. Consider the law of sines applied to the OBC triangle of figure 6(b):

$$\frac{OC}{\sin(\pi - \alpha_{By})} = \frac{OB}{\sin(\alpha_{Cy})} \tag{16}$$

leading to

$$m\gamma_C\sqrt{1+v_{Cy}^2}\,\frac{\sqrt{1+v_{By}^2}}{v_{By}} = m\gamma_B\sqrt{1+v_{By}^2}\,\frac{\sqrt{1+v_{Cy}^2}}{v_{Cy}}, \tag{17}$$

where we have taken into account that $\tan\alpha_{By} = v_{By}$ (see equation (4)), yielding $\sin\alpha_{By} = \frac{v_{By}}{\sqrt{1+v_{By}^2}}$ (and similarly for α_{Cy}). We have also used a simple generalization of equation (8) to find the expressions for OB and OC. Thus, after simplifying some factors, we recover equation (15).

We close this section with one last illustrative geometrical curiosity, albeit this one not in Minkowski momentum space. If we consider that $\mathbf{v}_B$ is fixed, we find from equation (15) the possible velocities $\mathbf{v}_C$ that can be obtained by adding a velocity along the x-axis to $\mathbf{v}_B$. This

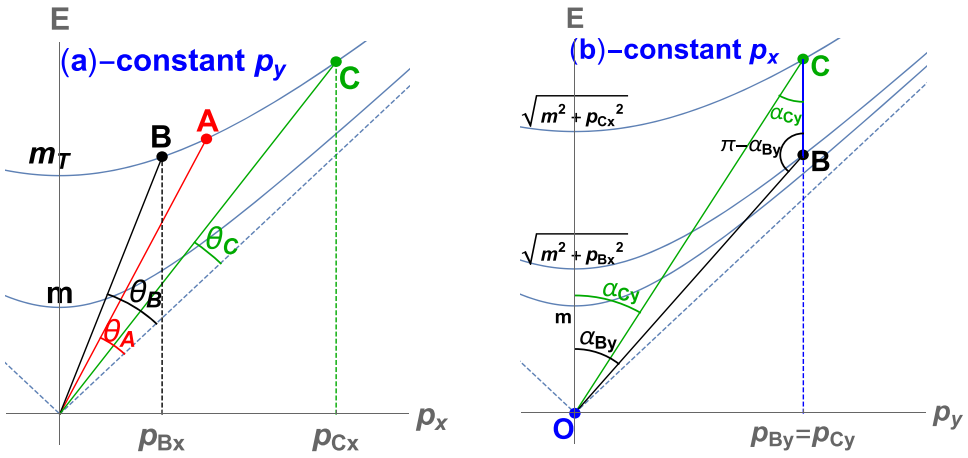

Figure 6. Plot (a) corresponds to a fixed p_y plane within the graph of figure 5. Taking into account that, in analogy with equation (4), $\tan(\frac{\pi}{4} - \theta_A) = v_A$, $\tan(\frac{\pi}{4} - \theta_B) = v_{Bx}$, $\tan(\frac{\pi}{4} - \theta_C) = v_{Cx}$, equation (7) still holds. The procedures of figure 2 or 3(a) can be applied here to find point C from A and B, but we do not depict them again. Knowing p_{Bx} and p_{Cx}, we can construct plot (b), where both hyperbolas are at constant (though different) p_x. Taking into account that (see equation (4)) $\tan\alpha_{By} = v_{By}$ and $\tan\alpha_{Cy} = v_{Cy}$, we see how changing p_x results in a change of v_y, a purely relativistic effect. In both plots we have included the hyperbola with its tip at $E = m$ ($p_y = 0$ and $p_x = 0$ respectively) in order to emphasize how having momentum in the transverse directions is in some aspects equivalent to having a larger mass.

turns out to be a semi-ellipse in the $v_{Cx} - v_{Cy}$ plane given by:

$$v_{Cx}^2 + v_{Cy}^2 \left(\frac{1 - v_{Bx}^2}{v_{By}^2} \right) = 1, \tag{18}$$

where v_{By} and v_{Cy} cannot have different signs. This is plotted in figure 7. The graph clearly shows that, as expected, when v_{Cx} approaches ± 1, one has $v_{Cy} \to 0$ in a way such that $|\mathbf{v}_C| \leqslant 1$. The maximum possible value of v_{Cy} is attained at the covertex of the semi-ellipse, when $v_A = -v_{Bx}$ such that $v_{Cx} = 0$.

4. Interactive applets

In order to complement the presentation of sections 2 and 3, we have developed a series of interactive dynamical geometry applets that can be found at [11].[9] The applets are based on the geometric constructions explained in the previous sections. The goal of these simple virtual laboratories is to help with the visualization of the concepts related to velocity addition and boosts, strengthening the learning process while engaging and motivating students [12]. This set of dynamic geometry apps has a didactic utility to explain typical concepts of relativistic kinematics and to solve problems associated with the change of inertial reference frame. In

[9] The apps and the eBook in which they are included were created using the free software resources available at http://geogebra.org.

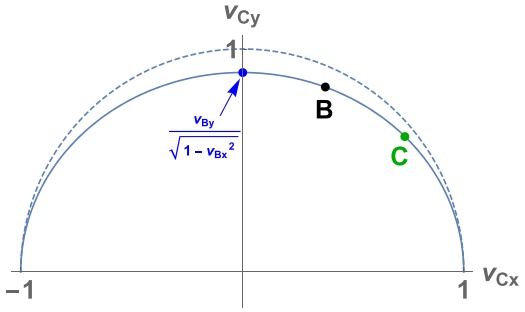

Figure 7. If we have a velocity $\mathbf{v}_B$ and perform a boost along the x direction with velocity $-1 \geqslant -v_A \geqslant 1$, the possible final velocities $\mathbf{v}_C$ form a semi-ellipse in the $v_{Cx} - v_{Cy}$ plane. The dashed line marks the speed of light. The depicted points B and C are the same as in the previous figures of this section. For a fixed B, the semi-ellipse is fixed and C would move to the different points of the ellipse as v_A changes (namely, as the red and green dots of figure 5 move along the hyperbola).

order to improve the possibilities of visualization, all these apps can be rotated and scrolled to observe the figures from the better suited perspective in each case.

The first applet corresponds to the resolution of the one-dimensional case of section 2, in which the two velocities to be added are collinear. The mass and momentum of the moving body and the velocity of the boost can be chosen by the user by clicking and dragging the corresponding dots within the figure. The auxiliary lines needed for the ruler-and-compass construction, the hyperbolic mass shell, and a horizontal velocity segment stretching from $v = -1$ to $v = +1$ are shown. It is interesting to observe how a boost with the speed of light stretches any (E, p) vector toward infinite energy and momentum along the mass shell hyperbola, without surpassing $v = 1$, in accordance with the postulates of special relativity. Even if the graphs are based on the geometric construction, the app can also be used as a numerical calculator, since it presents the values of both the selected variables and the result of the addition.

The second app corresponds to section 3, where collinearity of the two velocities/momenta is not required. Again, the mass and momentum of the particle and the speed of the boost can be freely chosen, and the app returns the resulting velocity and momentum in the $p_x - p_y$ plane. In addition, a three-dimensional view of the Minkowski space of momenta is also presented, where the geometrical procedure for the resolution is depicted. It involves a projection of the initial (E, p) vector on the plane of the boost, where the one-dimensional procedure is then applied. Then, the result is projected back onto the initial plane and we obtain the final result of the velocity addition. A color code for the points and their projections is introduced for the purpose of clarity. As in the one-dimensional case, this applet can also be used as a numeric calculator, since it displays the selected initial values and the results.

Finally, we have included a third app that allows the user to visualize a general boost in the three-dimensional space of momenta. In a sense, the $1 + 2$ dimensional case is the most general one since the $1 + 3$D case can be reduced to it by an appropriate rotation of the coordinate axes. However, we include this last case for the sake of completeness and because it provides further interesting visualization possibilities.

5. Conclusions and final remarks

Let us briefly summarize the main findings of this contribution. In section 2, we present several geometrizations of the velocity addition formula in $1+1$ dimensions, based on constructions in the energy–momentum plane. In particular, we have shown that $\tan\theta$, with the angle θ defined in figure 1(a) depends on the velocity in a way which can be directly connected to equation (2). The same is true for the length of the segment along the light cone from the origin to the projection of a (p, E) value (e.g. OA' in figure 2(a)) and, therefore, these projections are well-suited to establish a connection with the velocity addition formula. In figure 2 we show how this notion, together with Thales' theorem for similar triangles leads to a ruler-and-compass procedure to find the result of velocity addition. Then, two further ruler-and-compass methods are put forward in figures 3 and 4. They are remarkably simple ways of visually solving the addition of hyperbolic angles and, therefore, the relativistic addition of velocities.

Section 3 builds on the results of section 2 to generalise them to the case of non-collinear velocities. In fact, this is done in the spirit of dimensional scaffolding [16]: by gradually going up in the number of dimensions, conceptual complications are found sequentially, facilitating the learning process. In figure 5 we show that, graphically, the composition of velocities in $1+2$ dimensions can be reduced to the one-dimensional case by cutting the mass-shell hyperboloid along the appropriate plane. The resulting $1+1$ dimensional plane includes a hyperbola in which the tip corresponds to the transverse mass instead of the mass. Then, it also becomes clear from the plots why the velocity transverse to the boost is modified, even when the momentum remains fixed: the result of the addition will in general lie on a different hyperbola, as shown in figure 6(b). It is curious to see how the law of sines in the resulting triangle is equivalent to the known result of equation (15), depending on the relativistic γ factor. Let us also notice that generalizing the construction to $1+3$ dimensions introduces difficulties for the graphical visualization but, in fact, it does not introduce new conceptual issues since any pair of three-dimensional velocities can be brought to lie on the x–y plane by an adequate rotation of the Cartesian coordinates.

The purpose of this work has been the development of tools and strategies that can be applied in educational contexts in order to complement more standard approaches and provide an additional perspective. The geometrization of the velocity addition formula in connection to the energy–momentum plane and mass-shell hyperbolas and hyperboloids yields an interesting visual playground in which learners can work with several important concepts of special relativity, in connection with notions of trigonometry and Euclidean geometry. This auxiliary Euclidean geometry was built by choosing a particular reference frame in Minkowskian geometry, in which special relativity is naturally defined but which does not allow for the visual realizations developed here. Moreover, the interactive applets provide an entertaining but accurate visual implementation of the described solutions, and should contribute to the maturation of correct intuitions in the students who test them carefully. The author of [6] emphasized the pedagogical usefulness of Minkowski diagrams in momentum space when discussing particle interactions. We believe that our discussion shows that they can also be useful for the understanding and visualization of velocity addition.

Acknowledgments

We thank the anonymous referees for comments that have allowed us to greatly improve the presentation of this manuscript. This publication is part of the R & D & i project PID2020-118613GB-I00, funded by MCIN/AEI/10.13039/501100011033/. The work of AP has also

been supported by grants ED431B 2018/57, ED431B 2021/22 from Conselleria de Educacion, Universidade e Formacion Profesional and FIS2017-83762-P from Ministerio de Economia, Industria y Competitividad, Spain. JM is part of iMATUS - USC and of the Program for Consolidation of Research Units of Competitive Reference (GRC), supported by Xunta de Galicia.

ORCID iDs

Angel Paredes https://orcid.org/0000-0003-3207-1586
Xabier Prado https://orcid.org/0000-0001-9535-7499
Jorge Mira https://orcid.org/0000-0002-6024-6294

References

[1] Alstein P, Krijtenburg-Lewerissa K and van Joolingen W R 2021 Teaching and learning special relativity theory in secondary and lower undergraduate education: a literature review *Phys. Rev. Phys. Educ. Res.* **17** 023101
[2] Prado X, Domínguez-Castiñeiras J M, Area I, Paredes A and Mira J 2020 Learning and teaching Einstein's theory of special relativity: state of the art (arXiv:2012.15149) Pubished (in Spanish) in *Revista Eureka sobre Enseñanza y Divulgación de las Ciencias* **17** 1103 and Revista de Enseñanza de la Física 32 107–122
[3] Mermin N D 1997 An introduction to space-time diagrams *Am. J. Phys.* **65** 476–86
[4] Takeuchi T 2010 *An Illustrated Guide to Relativity* (Cambridge: Cambridge University Press)
[5] Dray T 2017 The geometry of relativity *Am. J. Phys.* **85** 683–91
[6] Saletan E J 1997 Minkowski diagrams in momentum space *Am. J. Phys.* **65** 799–800
[7] Bokor N 2011 Analysing collisions using Minkowski diagrams in momentum space *Eur. J. Phys.* **32** 773–82
[8] Prado X, Area I, Paredes A, Castiñeiras J M D, Edelstein J D and Mira J 2018 Archimedes meets Einstein: a millennial geometric bridge *Eur. J. Phys.* **39** 045802
[9] Brehme R W 1969 Geometrization of the relativistic velocity addition formula *Am. J. Phys.* **37** 360–3
[10] Kocik J 2012 Geometric diagram for relativistic addition of velocities *Am. J. Phys.* **80** 737–9
[11] Paredes A, Prado X and Mira J 2021 Interactive applets for velocity addition/boosts (https://geogebra.org/m/t87vpnup)
[12] De Jong T, Linn M C and Zacharia Z C 2013 Physical and virtual laboratories in science and engineering education *Science* **340** 305–8
[13] Rau M A 2017 Conditions for the Effectiveness of multiple visual representations in enhancing STEM learning *Educ. Psychol. Rev.* **29** 717–61
[14] Hatherly P A, Jordan S E and Cayless A 2009 Interactive screen experiments-innovative virtual laboratories for distance learners *Eur. J. Phys.* **30** 751
[15] Landau L D and Lifshitz E M 1971 *The Classical Theory of Fields* 3rd revised English edn (Oxford: Pergamon)
[16] Prado X and Mira J 2021 Dimensional scaffolding of electromagnetism using geometric algebra *Eur. J. Phys.* **42** 015204